A COMPUTATIONAL STUDY ON ION EXTRACTION FROM A LASER-GENERATED PLASMA USING A 2D PIC CODE

Dissertation submitted to Mahatma Gandhi University in partial fulfilment of the requirement for the award of degree of

Master of Science in Space

By

ALEENA PAULY

220011023277

Under the supervision of

DR.S. BARUAH & DR.B. DIKSHIT

ADVANCED TUNABLE LASER APPLICATIONS DIVISION

BHABHA ATOMIC RESEARCH CENTRE, MUMBAI

DEPARTMENT OF PHYSICS

BHARATA MATA AUTONOMUS COLLEGE

THRIKKAKARA, KERALA-21

MAY 2024

Beam Technology Development Group
Advanced Tunable Laser Applications Division
Quantum Computing & Process Diagnostic Section

Ref: BARC/BTDG/ATLAD/QCPDS/Training

Trombay, Mumbai 400085
30th April 2024

Sub: Certificate for completion of Training/Project Work

This is to certify that Ms. ALEENA PAULY, student of 2nd year MSc (Space Science) from Bharata Mata College, Thrikkakara, has successfully completed her training/project work on "Computational study on ion extraction from a laser-generated plasma using a 2D PIC code" during the period from 01/03/2024 to 30/04/2024 in Advanced Tunable Laser Applications Division of Bhabha Atomic Research Centre.

During this training period, she has got familiarised with a 2D Particle-In-Cell (PIC) code for plasma simulation and studied ion extraction process from a photo-plasma for predicting time duration required for complete collection of ions for a laser isotope separator system.

Ms. Aleena Pauly is a very enthusiastic and hard-working person. Her conduct and performance during this training period was found excellent.

Sudarshan Baruah

Dr. S. Baruah
SO/F

B Dikshit

Dr. B. Dikshit
Head, QCPD Section

डॉ. बी. दीक्षित / Dr. B. Dikshit
प्रमुख, क्वांटम कम्प्यूटिंग एवं प्रक्रिया निदान अनुभाग
Head, Quantum Computing & Proc. Diagnostic Section
एटीएलएडी, बीटीडीजी / ATLAD, BTDG
ट्रॉम्बे, मुंबई / Trombay, Mumbai-85

Bharata Mata Autonomous College
Department of Physics
Thrikkakara, Kerala

CERTIFICATE

This is to certify that the project entitled "A COMPUTATIONAL STUDY ON ION EXTRACTION FROM A LASER-GENERATED PLASMA USING A 2D PIC CODE" is a record of bona-fide work done by Ms. ALEENA PAULY (Reg. No. 220011023277) in partial fulfilment of the requirements for the award of Master's Degree in Space Science for the year 2022-2024 from Mahatma Gandhi University and no part of this work has been submitted earlier for the award of any degree.

DATE: DR. Shibi Thomas

PLACE: HOD, Department of Physics

External Examiner

Bharata Mata Autonomous College
Department of Physics
Thrikkakara, Kerala

DECLARATION

I, Aleena Pauly do hereby declare that the dissertation entitled "A COMUTATIONAL STUDY ON ION EXTRACTION FROM A LASER-GENERATED PLASMA USING A 2D PIC CODE" is a Bonafede record of the work carried out by me under the supervision of DR. S. Baruah & DR. B. Dikshit, ATLA Division, BARC, Mumbai during the year 2024 and it has not been submitted to any other University or Institution for the award of any other degree.

ALEENA PAULY

DATE:

PLACE:

ABSTRACT

Isotope of many atoms are now used in the field of nuclear medicine for the treatment and diagnostics of many deceases especially for cancer. ^{177}Lu is one of them with great demand for the treatment of prostate cancer and other targeted radionuclide therapy (TRT). This paper mainly aims to present the production of this particular isotope and its computational study. The production of ^{177}Lu isotope includes many steps. (1) atomic beam generation of Lutetium (2) enrichment of ^{176}Lu which act as a precursor for the production by AVLIS process (3) collection of ^{176}Lu isotope by applying an external electrostatic potential (4) treating the collected isotope with nitric acid followed by its analysis (5) irradiation of ^{176} Lu using neutron bombardment in nuclear reactor. Computational study of this ion extraction process is done by 2D Particle in Cell simulation method. We analyse the kinetics of plasma evolution using this technique and calculate the ion extraction efficiency of the process.

INDEX

CHAPTER 1

INTRODUCTION

1.1 Plasma and Radioisotopes

Plasma is the fourth state of matter and contains charged particles such as ions (positively charged) and electrons (negatively charged). The characteristic of plasma is that it obeys quasi-neutrality and exhibits collective behaviour. Quasi-neutrality comes from the fact that the total number of the positive and the negative charges are equal macroscopically. The coulombic interaction among the particles leads to collective behaviour of the plasma and affects the trajectory of motion of the individual particles. Plasma makes up 99.9% of the visible matter in the universe. Stellar interiors and atmospheres, gaseous nebulas, galaxies, core and corona of the sun and solar wind all contain plasma. Earth's ionosphere contains a small fraction of plasma. Van Allen Belt rings and aurora borealis are other examples of plasma around our planet resulting from the solar wind.

In the laboratory, plasma can be produced by various techniques. Heating a gas to a very high temperature results in the ionization of its atoms and molecules creating a plasma. Another way of generating a plasma is to use energetic photons (e.g., from laser) to ionize gas atoms or molecules. In fact, photoionization is the dominant process for plasma generation in space with the photons available abundantly from the nearby stars.

The plasmas, produced by various means, vary greatly in terms of density, temperature, stability and other characteristics. In case of the plasma produced by laser in typical isotope separator systems, density is ~10^8-10^{10} per cm^3 and temperature is about 2300 – 2900 K (~0.2 - 0.25 eV). To put this in perspective, solar plasma has a density of ~10^{26} per cm^3 (temperature ~10^7 K) and ~10^9 per cm^3(temperature ~10^6 K), respectively, in the core and the corona.

Here in our case, we consider a specialized plasma called photo-plasma generated by photo-ionisation process using tunable lasers. It has density in the range of 10^8 to 10^{10} cm^{-3} and low

temperature which makes the collective behaviour of plasma insignificant. Otherwise, the calculations became more complex and take more time to solve newtons equations of motion which is the main part of simulation. Ionization happens during the photoionization process, when incoming photons with energy equal to or higher than the absorbing atom's ionization potential are absorbed. The fundamental parameters that characterise photo-plasma are the density and temperature of each species. In addition to this Debye length, plasma frequency and other parameters which are explained in following sections.

Plasma has a wide range of application including medical and industrial. BARC in Mumbai deals with lower and higher temperature plasma and they developed many technological tools such as high-power plasma cutting torch, MHD generator, plasma spray coating of ceramic on metals and so on. This project focussed on the medical application of plasma that uses a radioisotope separated from laser produced plasma.

The unstable form of an element that emits radiation to change into a more stable form is known as a radioisotope. Radiation can alter the material it strikes upon and is easily traced. Because of these unique qualities, radioisotopes are used in industry, medicine, and other fields. In medical field the released radiation that may be picked up by medical imaging technology, enabling extremely fine-grained visualization of inside body systems and functions. This characteristic is essential to diagnostic processes, especially when recognizing, evaluating, and tracking different illnesses. Radioisotopes are also used therapeutically to treat a variety of illnesses, including cancer. In this instance, the radioactive component has a different function: it targets diseased cells with radiation, either killing or decreasing them while causing the least amount of harm to the surrounding healthy tissue.

Therapeutic isotopes (electron or alpha emitters) decay with half-lives in the range of minutes to hours, whereas isotopes used for diagnostic reasons (gamma or positron emitters) usually have durations ranging from days to weeks. Nuclear medicine demands a steady and sufficient supply of pertinent medical isotopes due to this ongoing loss through decay as well as the requirement to perform timely medical procedures for all patients in need. The production and delivery need for the used medical isotopes vary. For instance, isotopes having longer half-lives, such as lutetium-177 (^{177}Lu) and molybdenum-99 (^{99}Mo), are usually created in nuclear reactors through fission or activation and subsequently supplied to medical facilities all over the world. Shorter-lived isotopes must be created locally or delivered across shorter distances.

Reactor produced radioisotopes used for different therapies includes Iridium 192, Samarium 153, Iodine 131 where iodine used for both diagnosis and treatment of thyroid cancer. ^{153}Sm is for the cure from bone metastases pain and ^{192}Ir which supplied in the form of a wire for the treatment of certain types of cancer mainly heads and breast as a brachytherapy source. One of the widely used isotope Technetium-99m which has half-life of 6 days also produced in reactor and act as a tracer for SPECT (single photon emission computerized tomography) imaging of brain, bones, spleen, gallbladder, liver, blood pool, bone marrow and heart. Apart from this many cyclotrons produced isotopes are used for diagnosis process and our interest falls mainly on ^{177}Lu production which is used for prostate cancer treatment and targeted radionuclide therapy.

The worldwide usage of medically important radioisotopes mainly for cancer treatment increases its need that leads to the global production of these radioisotopes.

1.2 Why Lutetium 177

The Lutetium 177 isotope is widely used in targeted radionuclide therapy (TRT). It is a radioactive isotope with a half-life of 6.65 days. It decays to ^{177}Hf, producing β-particles with energies of 497 keV (76%), 384 keV (9.7%), and 176 (12%). ^{177}Hf, produced in nuclear excited states, decays to the ground state and emits low-energy γ-radiation with energies of 208 and 113 keV. ^{177}Lu has a mean β-particle penetration depth of 670 μm, making it effective for treating tiny cancers and lesions. Low-energy gamma photon emitted by ^{177}Hf are useful for imaging and the studies of biodistribution and excretion kinetics. The 6.65-day half-life of ^{177}Lu provides longer half-lives, which would be needed for radiolabelling and purifying ^{177}Lu-labeled radiopharmaceuticals. In addition to minimizing decay loss that could occur during transportation and user distribution, longer half-life offers excellent logistical advantages for shipment to locations far from both radionuclide processing facilities and reactor production facilities.

In the first widely utilization of^{177}Lu is for treating well-differentiated neuroendocrine tumours (NET), which would be originated from cells of the neuroendocrine system and is often found in the gastrointestinal tract and pancreas. Peptide receptor radionuclide therapy, or PRRT, is the term most commonly used to describe this treatment. Currently, ^{177}Lu-DOTATATE therapy is being investigated for a number of additional tumour types, such as thyroid cancer, melanoma, Merkel cell carcinoma, embryo neuroblastoma.

Prostate-specific membrane antigen therapy, or lutetium-177 PSMA Therapy, is gaining popularity as a treatment option for men with metastatic or treatment-resistant prostate cancers who have advanced prostate cancer. Prostate cell membranes express a protein called PSMA, which is thought to serve a variety of biological purposes. PSMA will be visible in such body parts if prostate cancer has spread to other regions. One treatment that uses radiation is lutetium, which attaches itself to the PSMA receptors on cancer cells using a chemical. Beta radiation, which is released by lutetium-177, efficiently damages and eventually kills cancer cells. Lutetium's radiation-focused therapy becomes extremely accurate by focusing on the PSMA molecules since it attaches to them. Peptide Receptor Radionuclide Therapy (PRRT) is the term commonly used to describe the process of specifically targeting cancer cells.

1.3 Production of Lu 177

For targeted radiation, lutetium-177 (Lu-177) has shown promise as a short-range beta emitter. The demand for Lu-177 has increased significantly. In India Lu-177 is produced in Druva nuclear reactor at Baba Atomic Research Centre (BARC), Mumbai by subjecting the source material to neutron (n, γ) radiation. There are now two methods available for producing Lu-177. The first is the Carrier Added (CA) approach, which uses Lu-176 as a source material; the second is the Non - Carrier Added (NCA) method, which uses enriched Yb-176 as a nuclear reactor source material. Both have its own advantage as well as disadvantage. In the first approach, lutetium must be enriched in ^{176}Lu to increase yield of ^{177}Lu and avoid generating undesirable other radionuclides. One milligram of enriched lutetium is required to produce about 50 patient doses by this approach, which has the initial benefit of a high chance of nuclear reaction. Another benefit is that the only radiochemical processing that occurs after irradiation is the comparatively straightforward production of lutetium chloride. This path has a few disadvantages as well. Only over 30% of the lutetium remains radioactive 177Lu after irradiation. By the time it reaches the patient, there is less usable lutetium because the remaining lutetium is stable while the ^{177}Lu decays. This route's other disadvantage is that, in addition to producing ^{177}Lu, the irradiation also produces some ^{177}mLu, an undesired beta emitter with a long half-life of 160 days that presents other difficulties, such as waste management.

The main obstacle to producing ^{177}Lu through direct irradiation of natural Lu is the low natural abundance (2.59%) of its precursor Lu 176. In order to achieve the necessary isotopic purity and high specific activity of Lu-177, the lutetium sample to be irradiated must be en-

riched in Lu-176 from its native abundance of 2.6% to usually better than ~ 80%. One of the most effective and profitable methods for isotope enrichment is Atomic Vapor Laser Isotope Separation (AVLIS). The natural Lu is first put into a crucible, where it is melted by irradiation of an electron beam to produce atomic vapour. This vapour then heads towards the

collimators with small divisions where it interacts with a pulsed laser beam that selectively ionizes Lu 176 only, forming a finite-sized photo-plasma in the interaction zone. Finally, the enriched Lu 176 isotope is collected by the application of an external electrostatic field. The collected 176Lu ion is treated with nitric acid to separate the isotope from collector plate. After the analysis of the quantity and quality of isotope it is given to Druva nuclear reactor in BARC where the irradiation with neutron results in Lu-177 isotope.

The main objective of this work is to study the process of ion extraction from the laser generated plasma. The computational study is done by an in-house developed 2D Particle in Cell (PIC) code. Collection efficiency of ions, time duration for collection process and required electric field can be deduced by using this 2D PIC code.

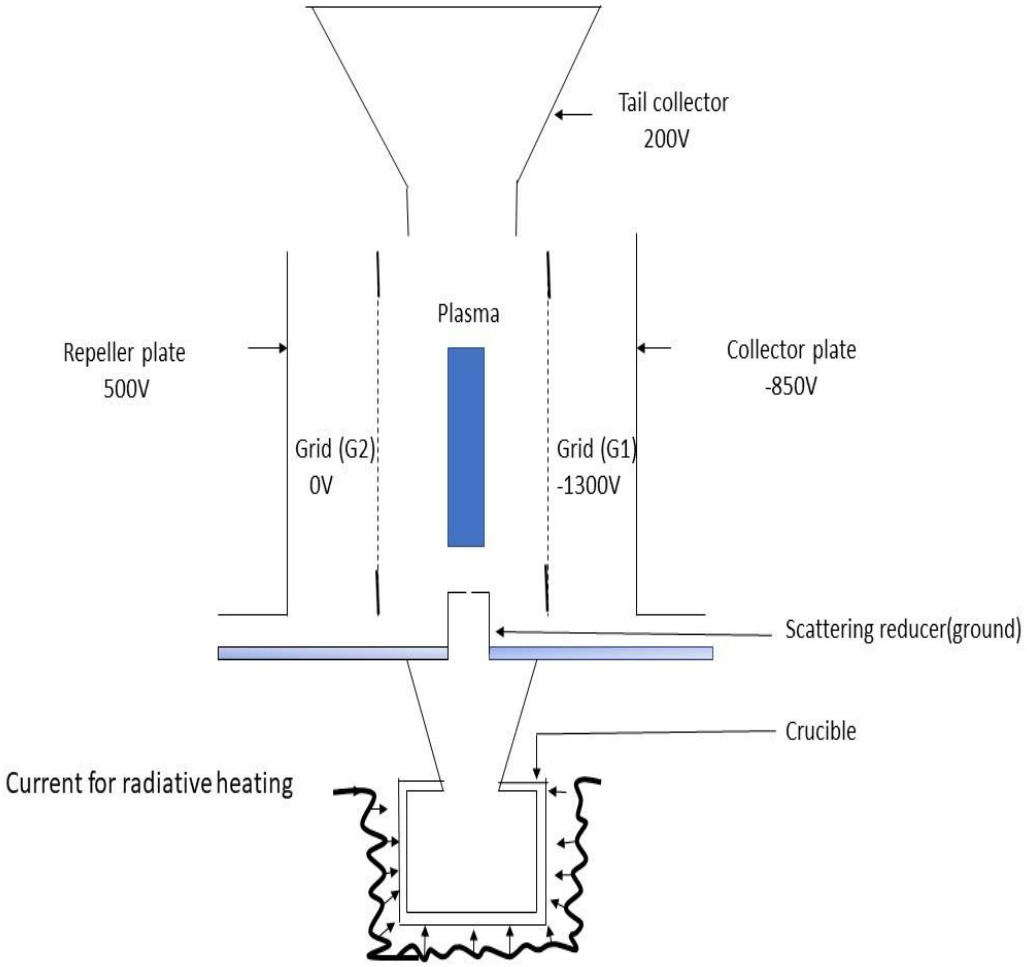

Fig 1.3.1: 2D schematic diagram of the ion extractor assembly for the separation of Lu 176 isotope [1,3]

CHAPTER 2

EXPERIMENTAL SETUP

2.1 Production of atomic vapour

For an efficient AVLIS process it is desirable to generate atomic beam of required density(~10^{12}/cm^3) with narrow doppler width at the laser interaction zone. First, natural Lutetium is melted and then evaporated at about 1800 - 1830 ℃ in a crucible provided with a collimating slit. Melting and evaporation can be done by electron bombardment method with a heating coil/filament made of tantalum or tungsten which surrounds the crucible. The crucible is kept at ~2 kV so that electrons are drawn to it and bombard it at a kinetic energy of 2 keV. The filament temperature is raised to roughly ~2100℃ to cause thermionic electron emission. By using this technique, the crucible receives power from electron bombardment as well as heat radiation from the filament. The issue with this technique is to maintain a good vacuum at all times to prevent electrical discharges and to keep the high temperature crucible electrically insulated so that it can withstand 2 kV of voltage. Evaporated atoms interact with the laser beam where the selective photo ionisation process takes place.

2.2 Photo-plasma Generation

Atomic Vapour Laser Isotope Separation uses high power high repetition rate tunable lasers for selective ionization of the desired isotope, which results in the formation of a plasma containing ions of the desired isotope. Dye lasers, pumped by diode pumped solid state lasers (DPSSL) and copper vapour lasers (CVL), are used for photo-ionisation. Lutetium has two naturally occurring isotopes, both having hyperfine structures: Lu-176 (2.59%) and Lu-175 (97.41%). A three-step three-wavelength isotope selective photoionization technique that provides the best possible selectivity and yield of the product has been developed at ATLA Division, BARC. A combination of three laser beams interacts with the atomic vapour in a multi-pass fashion using a group of mirrors in order to extend the interaction volume. The electronic structure of Lu has two transitions from ground level where laser is available:

540nm and 573nm. A 573 nm tuned laser (DL-1) is used as the starting point of the photo-ionization ladder to excite the Lu atoms from ground level to 17427.28 cm-1 (F =17/2 to F'=17/2). The pulses from DL-1, DL-2 and DL-2, DL-3 lasers have optical delays of 10 ns and 2-3 ns, respectively, so that the pulses arrive at the laser-atom interaction zone successively.

DL-2 is tuned to 609nm, while the wavelength of DL-3 ionizing laser is optimized at 570nm for the Lu-176 ion signal. It is to be noted that at greater intensities, due to power broadening of laser, ionization of the unwanted isotope Lu-175 increases, that decreasing overall enrichment of the desired isotope. To reduce this effect, the laser intensities have to be adjusted to their optimised level. Multi-mode lasers with a typical line width of around 2GHz were utilized in this process. The three-step selective photo-ionization scheme is illustrated in fig 2.2.1,

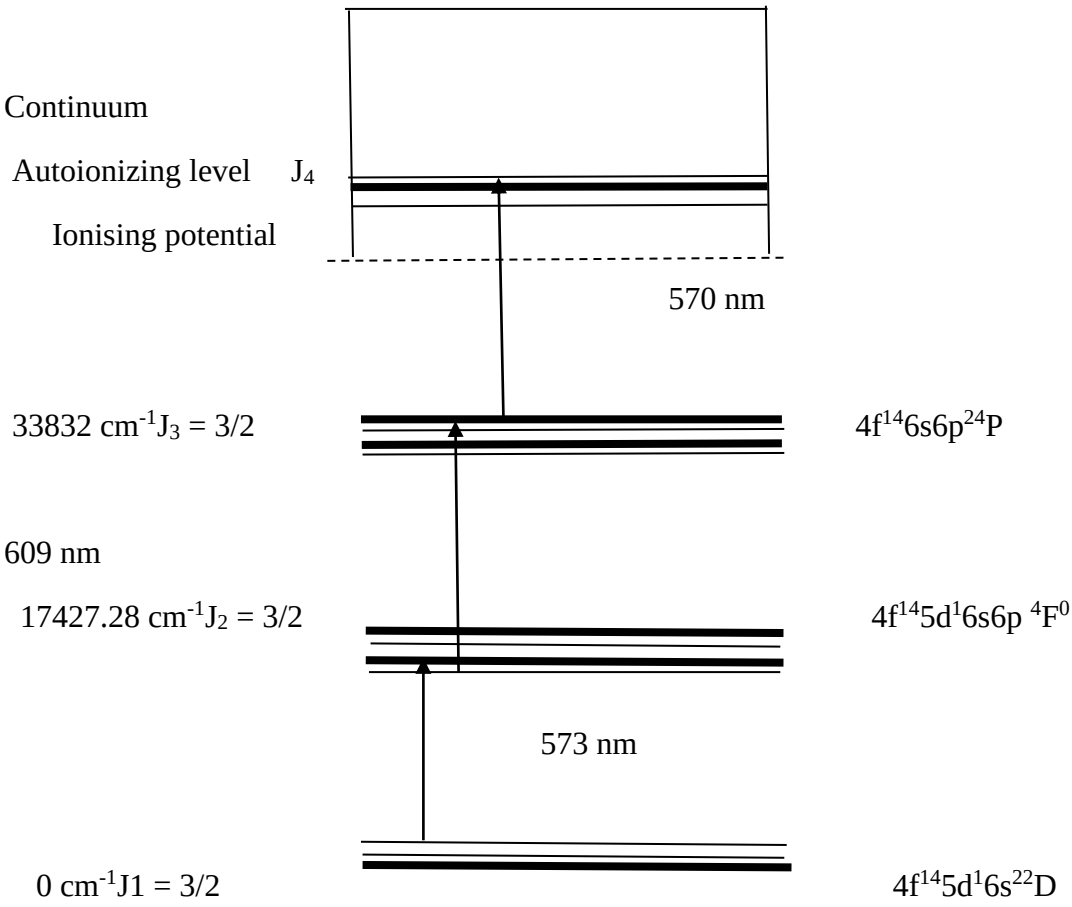

Fig.2.2.1: Schematic of the highly selective three step photoionization [7]

2.3 Major Plasma Characteristics

2.3.1 Debye length for spatial grid

Debye shielding is the ability of plasma to shield out applied electric potential. To understand this distinct behaviour, we examine a test positive charge that has been intentionally submerged in a thermally balanced plasma. At first, the velocity of the particles is extremely slow, and temperature has no bearing. The mobility of the particles increases with a gradual increase in temperature. Electrons go toward positive charge by forming a cloud there, while ions are repelled. At least for a brief while, the application of an external test charge disrupted the quasi-neutral behaviour of plasma. The Debye length is the radius of the Debye sphere, which forms as a result of the electron's random motion (thermal kinetic energy) and the potential pull of an externally applied charge. At some point, kinetic and potential energy equalize, and this is the maximum length of the sphere. In actuality, the electrons work to prevent the other plasma particle from being penetrated by the applied charge field. To separate the isotope Lu 176 in our case, we also used an external electrostatic field. The Debye length equation is provided by,

$$\lambda_D = \sqrt{\frac{\varepsilon_0 T_e(eV)}{ne}} \quad (1)$$

This relationship indicates that the temperature of the electron and the density of the plasma are the key determinants. The Debye sphere has a comparatively small number of particles when the density of plasma increases, but when temperature rises, the maximum Debye length is reached at a farther point, causing the Debye sphere to grow. Here in our case, electron density and temperature are assumed to be constants. The domain of the spatial grid is determined by using Debye length.

2.3.2 Plasma Oscillation

Relatively less massive electrons are moved from their mean position and move in the opposite charge when an external field perturbs the plasma. It tends to return to its starting location because of the restoring force, but inertia causes it to go farther before returning. As a result, the electron oscillates at a frequency known as plasma frequency, which is determined by an equation that also takes into account the Debye length and electron thermal velocity,

$$\omega_{pe} = \frac{v_{Te}}{\lambda_D} \quad (2)$$

The corresponding time period (τ_e) is the time within which the plasma responds to any external field and it is given by,

$$\tau_e = 2\pi\sqrt{\frac{\varepsilon_0 m_e}{ne^2}} \quad (3)$$

Where m_e is the mass of electron. Electrons attempt to shield the plasma from external fields by responding quickly to fields with frequencies lower than the plasma frequency. Therefore, in plasma modelling, the timestep needed must be smaller than the duration of the plasma oscillation. The time step's recommended value is $0.25/\omega_{pe}$. Other parameters of important are density of macroparticles, electron temperature (T_e) which determine the plasma expansion on free space and generally taken as 0.25eV, drift velocity of ions, mass and charge of macroparticles.

Plasma Parameters	Values
Plasma density	$5 \times 10^8 cm^{-3}$
Plasma frequency	$1.26 \times 10^9 rad/s$
Debye length	$0.4mm$
Electron temperature	$0.25eV$
Drift velocity of ion	350 m/s
Ion temperature	$0.02eV$
Ion mass	$176u$
Time Period	$5 \times 10^{-9} s$
Time steps	2×10^{-10}s

Table 1: Plasma Parameters used for computational study of ion extraction process of Lu-177

CHAPTER 3

COMPUTATIONAL STUDY OF ION EXTRACTION PROCESS

3.1 Particle in Cell (PIC)

Particle in cell is a widely used method for the simulation of charged particle dynamics. The core of this method is discretization of a continuous domain using spatial grid points and thereby calculating the charge density and electric field at nodes of grid whereas the velocity and position of charged particle takes continues value. Plasma modelling is complicated by the presence of external and self-induced electromagnetic fields, inter-particle interactions and the distinct time scales at which ions and electrons move. To speed up the calculation, simplifying assumptions that are appropriate for the problem at hand are typically used. We are presuming that the plasma medium generates a low enough current to ignore the self-induced magnetic field. As a result, the set of underlying Maxwell's equations is minimized, and we get an Electro-Static PIC code. We also suppose that the Boltzmann connection applies to electrons. At that point, the only particles in the simulation are heavy particle like ion and neutrals. Because the time integration may now be carried out on the considerably larger ion time scale, this simplification has a significant influence on computational speed. Lastly, we assume that particle collisions are insignificant due to low enough gas concentrations.

The coulombic interaction between plasma molecules is given by $F = \frac{1}{4\pi\varepsilon_0} \times \frac{q_1 q_2}{r^2} \times r_{12}$. For the simulation of motion of charged particle we have to consider coulombic interaction between every single particle in plasma and plasma simulation generally require at least one million particles in order to reduce numerical errors. A single time step would require at least 1 trillion operations to compute because Coulomb force results in a n^2 problem. Introducing particle in cell method uses a computational particle (also called super particles /macroparticles) to represent the real ions electrons and neutrals. Each computational particle

represent large number of real particle and they have charge to mass ratio equals to the original charge to mass ratio value. The ratio of real particles per macroparticle is called specific weight. Newton's Second Law of Motion governs the motion of every macroparticle:

$$\frac{dy}{dT} = \mathrm{v} \tag{4}$$

$$\frac{dV}{dT} = \frac{q}{m}E \tag{5}$$

In this case, m denotes the particle mass and q the particle charge. The formula for computing the electric field is $\vec{\ }\mathrm{E} = -\nabla\phi$, where ϕ represents the electric potential. It is provided by the Poisson equation, $\nabla^2\phi = -\rho/\epsilon_0$. Here, $\epsilon_0$represents the permittivity of open space and ρ represents the charge density. The charge density is expressed in terms of electron and ion number densities, or $\rho = e\,(Z_i n_i - n_e)$. The average ion charge number is represented by Zi, and the subscripts i and e stand for ions and electrons, respectively.

3.2 Principle of PIC algorithm

PIC algorithm contains initial setup, the main loop and final clean-up/output. The initialisation includes setting up the simulation's settings, defining geometry of model and grid parameters and creating the particles. The main loop has seven following steps,

1. Compute charge density: computing the charge density in every cell using particle weighing method and distributing the results among the grid nodes.
2. Compute electric potential: to be done by solving Poisson's equations.
3. Compute electric field: to be find by taking gradient of electric potential.
4. Move particles: integrating equation of motion of each particle updating and replacing the velocity and position of them.
5. Output: save the information on the state of simulation.
6. Repeat: iterate until maximum number of steps is achieved.

Schematic diagram of the loop is given below,

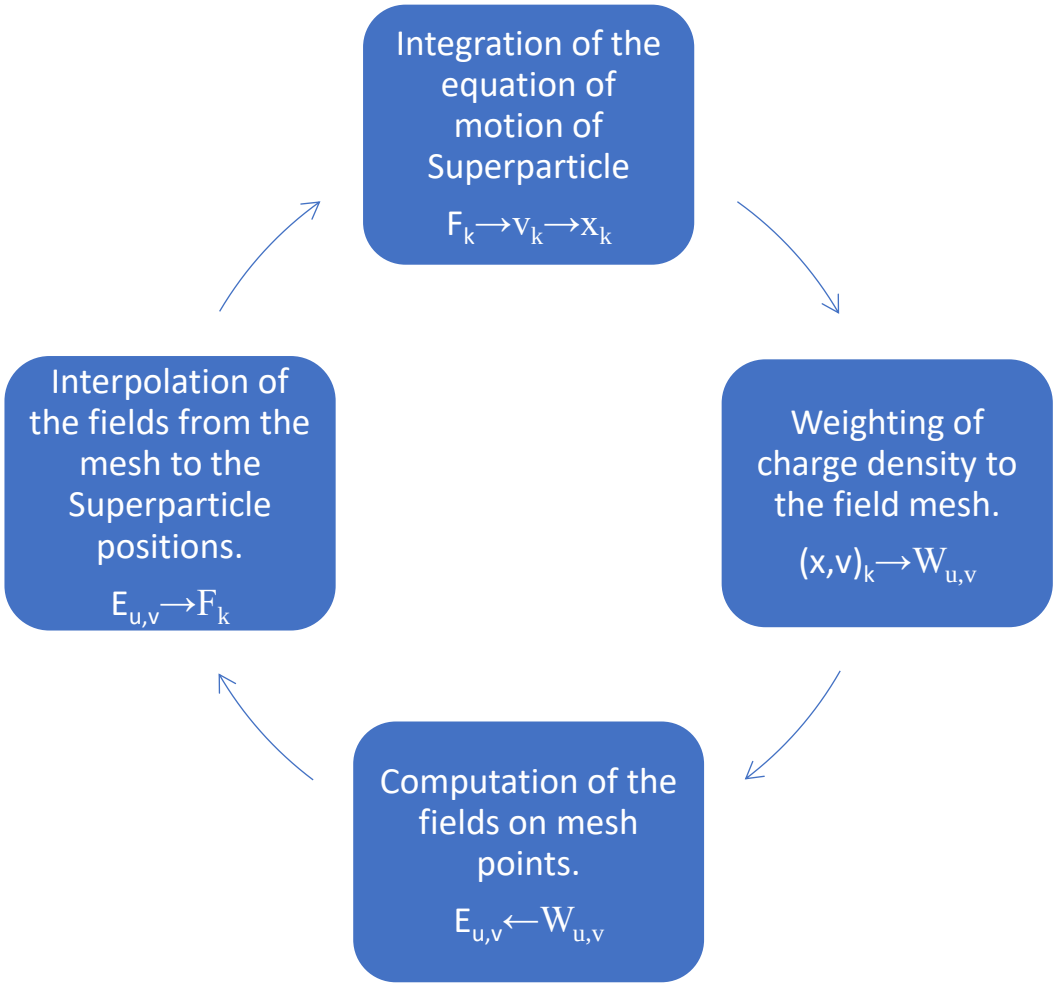

Fig.3.2.1: Schematic diagram of PIC algorithm [6]

3.2.1 Computation of charge density

A certain cell in a spatial grid that houses a collection of particles. According to Poisson's equation to find the potential at one node of grid the charge density at that node due to charge which is located somewhere in cell should be known. Charge density can be calculated using a method called first order interpolation weighting of particle where we assigning partial charge to four nearby nodes. For example, consider a charge q_p which is located at (r, s) position in 2D cell and let us take each node of this cell as (u,v),(u+1,v),(u+1,v+1),(u,v+1).We must calculate an appropriate weight or fraction and multiply it by the charge in order to assign a portion of the charge. The following is the procedure for calculating weights: the charge is localized in one vertex of each of the four smaller areas that we divide the cell's complete area into. Consequently, each area is a portion of the cell's total area. Let us try to find fraction at the grid point (u, v) in our example. For that take the opposite area $A_{u,\,v}$ and divide it by whole cell area A.

$$W_{u,v} = \frac{A_{u,v}}{A} = \frac{(h-r)\times(h-s)}{hh} \quad (6)$$

where (r, s) -position of particle, h -width and height of the cell. Weight is usually in between 0 and 1, multiplying the value with the particle charge will give partial charge $q_{u,v}$ at (u, v) node.

$$q_{u,v} = W_{u,v} \times q_p \quad (7)$$

similarly, the particle charge at other nodes is given as follows,

$$W_{u+1,v} = \frac{A_{u+1,v}}{A} = \frac{r\times(h-s)}{hh} \rightarrow q_{u+1,v} = W_{u+1,v} \times q_p \quad (8)$$

$$W_{u+1,v+1} = \frac{A_{u+1,v+1}}{A} = \frac{r\times s}{hh} \rightarrow q_{u+1,v+1} = W_{u+1,v+1} \times q_p \quad (9)$$

$$W_{u,v+1} = \frac{A_{u,v+1}}{A} = \frac{(h-r)\times s}{hh} \rightarrow q_{u,v+1} = W_{u,v+1} \times q_p \quad (10)$$

The sum of all four weight should be equal to 1. If there are multiple particles in this cell, then each particle should go through this process, and the weighted partial charge that results should be added to that specific node,

$$q_{u,v}^{Tot} = \sum_{n=1}^{N} q_{u,v}^{n} \quad (11)$$

where $q_{u,v}^{n}$–nth particle partial charge at (u, v) node.

This indicates that each cell node contains the total weighted partial charges contributed from each particle in this cell. For each cell in the domain, the same procedure must be followed. The calculation of charge density involves dividing the net charge at a certain node by the cell area (in a 2D example).

$$\rho_{u,v} = \frac{q_{u,v}}{A} \quad (12)$$

3.2.2 Computation of electric potential

For the calculation of potential of super particle's initial distribution at the nodes of spatial grid the Poisson's equation should be discretised to transfer it from infinite differences to finite ones using finite difference method with central differencing as follows,

$$\frac{\phi_{u-1,v}-2\phi_{u,v}+\phi_{u+1,v}}{h^2} + \frac{\phi_{u,v-1}-2\phi_{u,v}+\phi_{u,v+1}}{h^2} = -\frac{\rho_{u,v}}{\varepsilon_0} \quad (13)$$

There is a system of nonlinear equation is obtained simultaneously for different nodes of the spatial grid and it is solved by using relaxation method of iteration and finally get the potential at each node of the spatial grid.

3.2.3 Computation of electric field

The electric field $\boldsymbol{E}$ at the nodes of grid can be calculated using the following relation when the potential ϕ is known:

$$E = -\frac{\Delta\Phi}{\Delta r} \tag{14}$$

Expressions for E components interior nodes and boundary nodes can be generated by rewriting into a numerical form and applying the central difference scheme (12) and forward/backward difference scheme (13) to achieve the results.

$$E^{x}_{u,v} = -\frac{\Phi_{u+1,v} - \Phi_{u-1,v}}{2h} \quad E^{y}_{u,v} = -\frac{\Phi_{u,v+1} - \Phi_{u,v-1}}{2h} \tag{15}$$

$$E^{x}_{0,v} = -\frac{\Phi_{1,v} - \Phi_{0,v}}{h} \quad E^{y}_{u,0} = -\frac{\Phi_{u,1} - \Phi_{u,0}}{h} \tag{16}$$

Next, using an interpolation approach, the electric field at the neighbouring nodes is used to derive the electric field at the position of super particle. Multiplying E by the electric net charge (q), one may easily get the electrostatic force (F) and this force move particles to new position.

3.2.4 Move particles

Next, we have to update the new position and velocity of macroparticle by integrating the equation of motion of them using an implicit Leap Frog method through a time step Δt. For that the time domain must be discretized started at t_o and divided into uniformly spaced time points t_i, where $t_i = t_0 + i\Delta t$ (i=1,2,3...n) and $\Delta t = t_1 - t_0 = t_2 - t_1$ and so on, representing the size of each time step. The value of position x_0 and velocity v_0 at the initial time t_0 are known to us from the initial condition. From that values position of particle is evaluated at the end points of the time points (at t_1, t_2, t_3….) whereas velocity is evaluated at midpoint of the time points (at $t_{1/2}$, $t_{3/2}$, $t_{5/2}$….) in order to achieve second order accuracy. In other words, x and v are staggered so that they "leapfrog" over each other, as illustrated in the figure.

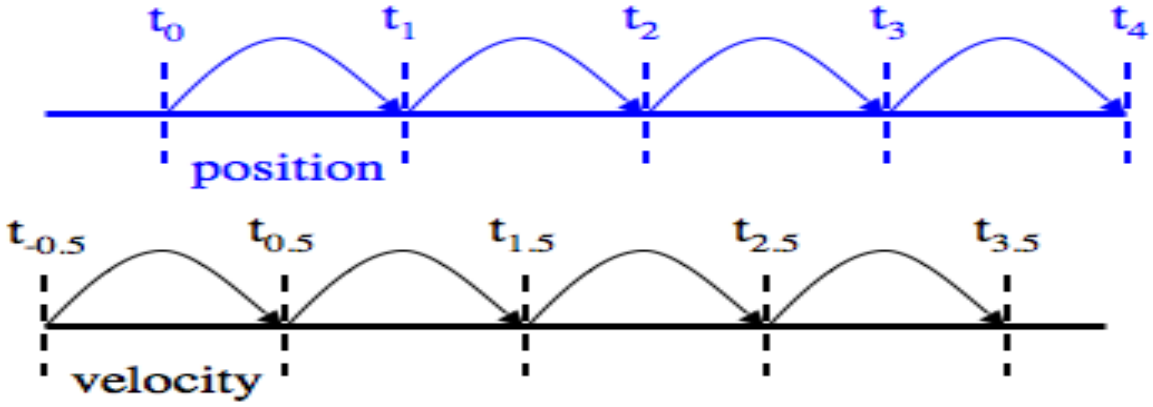

Fig.3.2.2: Schematic diagram of Leap-Frog method [10]

x and v are calculated numerically by leap frog method is given by

$$x_{i+1} = x_i + v_{i+1/2} * \Delta t \quad (17)$$

$$v_{i+1/2} = v_{i-1/2} + (qE/m) * \Delta t \quad (18)$$

Nevertheless, in order to start the Leapfrog scheme, we need to specify v ($t = t_0 - \Delta t/2$) = $v_{-1/2}$ in equation. Therefore, we evaluate $v_{-1/2}$ from the specified v_0 for the initiation using Euler's scheme. From the Euler's scheme,

$$v_{-1/2} = v_0 - (\Delta t/2) * (qE/m) \quad (19)$$

The Leapfrog method is fast, numerically stable and outperforms the Euler's scheme but falls short of the Runge-Kutta 4th order system in terms of accuracy. It's important to confirm that every particle is still inside the computational domain after moving them to new locations. There could be two interactions at the boundary. The particles may clash with solid objects or they may leave the domain.

3.2.5 Output and Repeat

Output from PIC codes include particle data such as velocities and current densities, as well as the spatial distribution of plasma parameters such as potential, charge density, and electron temperature. The loop is repeatedly carried out over a number of thousand-time steps until the simulation reaches the desired plasma dynamics.

3.3 2D PIC CODE

The in-house developed 2D PIC code is used to simulate the momentary evolution of discrete sized photo plasma at a cross-sectional plane of ion extractor geometry. The code is has an electrostatic field solver and is written in C++. The input parameters required for running the code is given in Table 1.

CHAPTER 4

RESULTS AND DISCUSSION

A finite sized laser generated plasma in the form of a rectangular slab of dimension $1cm \times 4cm \times 15cm$ is subjected to an external electric field using an extractor setup as shown in figure 1.3.1. The collector plate is kept at a voltage of -850V and placed at a distance of 75mm from the plasma in order to avoid collection of unwanted isotopes from the atomic vapour. A grid is placed between the plasma and the collector plate and kept at -1300V to initially accelerate the ions from the plasma towards the collector plate through the grid. The wires on the grid have 0.5mm diameter and the grid has a geometrical transparency of 90%. Between the grid and the collector plate, the ions undergo deceleration and lands on the collector plate with an energy around 850 eV. On the other side of the plasma, another grid is kept at 0V which lets the electrons pass through it towards the repeller plate kept at 500V. The tail collector is kept at 200V, and it helps to prevent ion loss due to overall upward flow. Bottom plate is grounded which reduces scattering of the atomic beam. A computational domain with a dimension of $240mm \times 208mm$ is created for the simulation with Dirichlet boundaries (0V). For the given plasma density of $5x10^8$ per cm^3, time-step duration is taken to be $2x10^{-10}$ ($=0.25/w_{pe}$) second and the cell length along X and Y is taken to be 0.2mm (=Debye length). The simulation is run for a time duration of 10 microseconds so that all ions are collected and removed from the simulation domain.

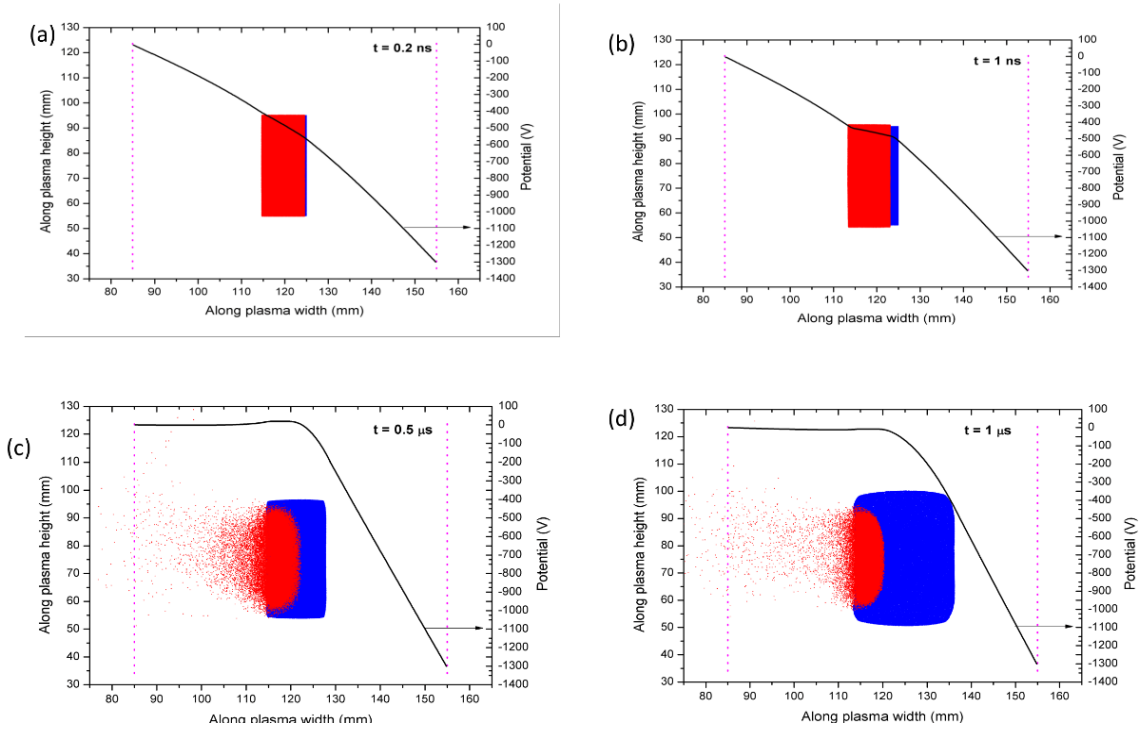

Fig 4.1: Spatial variation of plasma potential along x axis for a constant y at (a) t = 0.2ns (b) t = 1ns (c) t = $0.5\mu s$ (d) t = $1\mu s$

Fig 4.1 shows the distribution of plasma potential and the corresponding electron ion movement upto $1\mu s$. The dotted lines show the location of the repeller side grid (kept at 0V) and the collector side grid (kept at -1300V), respectively. The plasma potential curve (in black) corresponds to the Y-axis on the right side of each plot. Fig 4.1 (a) corresponds to the state just after one simulation time-step and shows the profile of the potential due to the extrenally applied voltages. The electrons are shown with red dots and the ions are shown with blue dots. As the electons and ions start separating and form an ion sheath on the right side of the plasma, the potential at the location of the plasma starts to increase. The potential increases from an initial ~ -500V to ~30 V at 0.5 microsec. Beyond that time, as the ions start expanding, the ion density falls and the gradually the potential starts to decrease again before attaining the original value after about 7 – 8 microseconds. This is evident in Fig. 4.2 where the potential curves are plotted for different times of the plasma evolution. The two dotted vertical lines here represent the width of the plasma (10 mm).

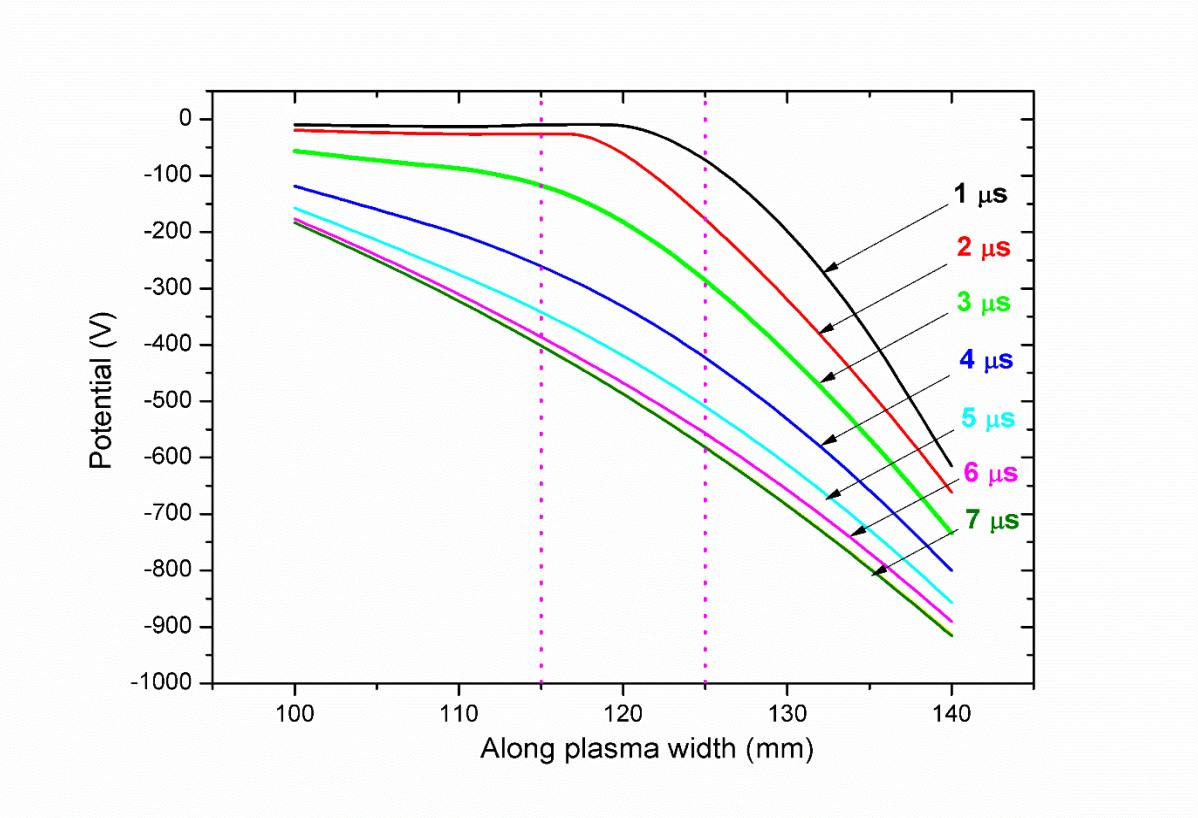

Fig.4.2: Spatial variation of potential of plasma at every micro seconds

To study the evolution dynamics, we analyse the 2D spatial profiles of the electrons and the ions at different time-steps in Fig. 4.3.

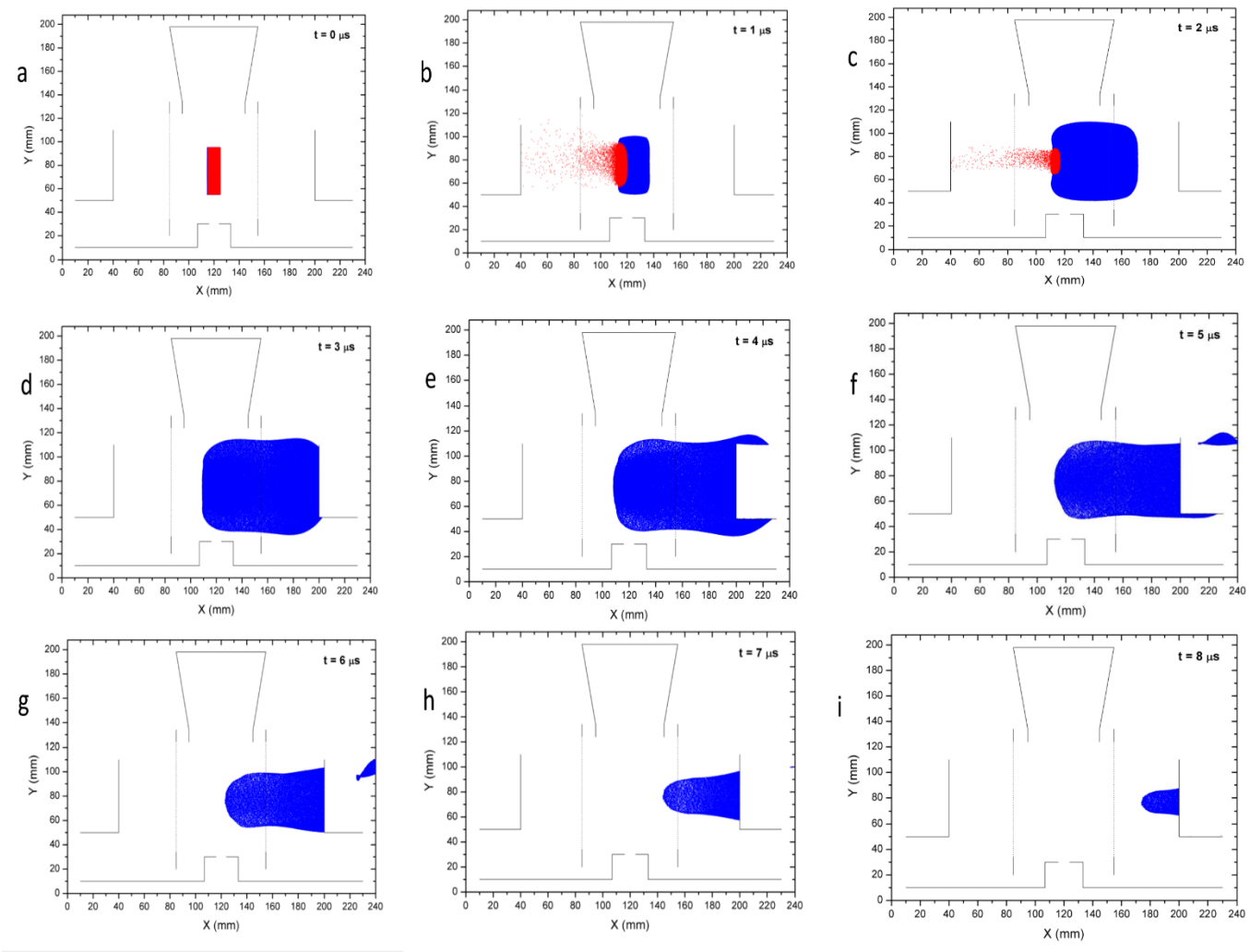

Fig 4.3: Spatiotemporal evolution of plasma at (a) t = $0\mu s(b)\ t = 1\mu s(c)t = 2\mu s(d)t = 3\mu s(e)t = 4\mu s\ (f)t = 5\mu s(g)t = 6\mu s(h)\ t = 7\mu s(i)t = 8\mu s$

Fig 4.3 (a) shows the plasma at initial timestep t = $0\mu s$. Immediately afterwards, the seperation of charges start giving rise to an ion sheath towards the grid on the collector side. The electron starts moving towards the repeller plate through the left-side grid. Had there been no plasma effect, electrons collection whould have been complete in a few nanoseconds, but due to the plasma effect, although not very strong in this density, electrons take up to a few microseconds to get completely removed from the simulation. The ions motion is slower compared to the electrons due to their higher mass value. Although the ions start their motion towards the collector grid in a conversing fashion, after crossing the grid, they start to diverse in the upper and lower boundaries as they face a deccelerating electric field between the grid and the collector plate. This contributes to some loss of ions as can be seen in the plot of 4 microseconds onwards. This loss becomes more significant at higher plasma densities. The interception at the grid wires also contribute to ion loss, which can go up beyond 15% for

high density plasma due to back and forth ion oscillation between the collector plate and the gird. The electron and ion currents are plotted in Fig. 4.4. As seen from the curves, electrons are collected quickly with the process completing within 2.5 microseconds but the ion currrent starts about 2.8 microseconds and extends up to about 9 microseconds. It is to be noted that the ion current rises sharply but falls in a gradual manner. The currents are plotted in arbitray units only to give a comparison of magnitude between the electron current and the ion current. The estimation of actual magnitude of ion or electron current requires 3D simulation and with the current computational resources, it will take several months for such a simulation to complete. The plot shows the extraction current after one pulse of laser. As the repition rate of the laser pulses is 12.5 kHz, the time duration between two laser pulses is 80 microseconds. Thus, there will be 7,50,000 such extraction signal pulses in a duration of 1 minute.

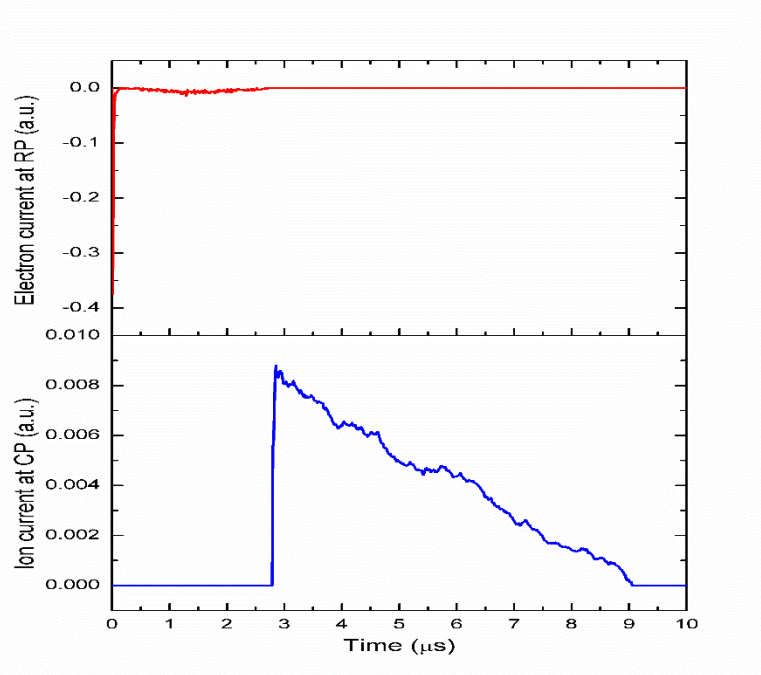

Fig 4.4: Electron-ion current v/s time

From the area under the ion current vs. Time plot, we can calculate the number of ions reaching the collector plate, from which we can also deduce product collection rate in mg/hour. We can calculate ion extraction efficiency of this process by taking ratio of the number of ions reaching the collector plate to the initial number of plasma ions taken for simulation. For our current simulation, ion collection efficiency is found to be ~70%.

CHAPTER 5

CONCLUSION

A computational study of photo-plasma after the enrichment of ^{176}Lu is done by using the two-dimensional electrostatic PIC simulation. The configuration for the ion extraction process consists of photo-plasma, G_1 and G_2 grids, repeller and collector plate, tail and bottom plate. The dynamics of plasma is studied from spatiotemporal evolution of plasma and electric potential plots. From the electron ion pulses it is clear that electron current is maximum at $0.5\mu s$ and there by decreases. Similarly, ion current is maximum at $\sim 3\mu s$ thereby falls. At some point the two currents become stable also. Collection of ions completed $\sim 9\mu s$ time. This study gives me the idea of ion extraction process behind medical isotope separation of ^{176} Lu and its computational study.

The collision between the particle became significant if the density and temperature of plasma increased. There are different types of collision occurs inside the plasma. The charged-neutral collision and columbic collision which may or may not change the direction and kinetics of plasma which makes the process more complex. In addition to PIC method, we have to implement Monte-Carlo simulation method for computational study of collisional plasma. MC method uses the random number generation to specify the collision of each particle.

ACKNOWLEDGMENT

First and foremost, Praises and thanks to God Almighty, the creator, for the blessings throughout my project work to complete the dissertation work successfully.

I am greatly indebted to DR.S. Baruah & DR.B. Dikshit, ATLA Division, BARC for the blessings, scholarly guidance, valuable advices, and constant encouragement, throughout the course of my project work. I learned lot of new things from them scholarly and behaviourally.

I extend my gratitude to Group director, Divion head, Section head, ATLA Divion, BARC, and all other scientist of the division for their advice, support, help and encouragement throughout my project work.

I would like to express my sincere thanks to my tutor Dr. Manesh Michael for providing facilities and resourceful academic environment needed for my project work.

I wish to express my heartfelt and sincere gratitude to Dr. Shibi Thomas, Head of Physics Department for her encouragement and support during the time period of this project.

I would like to express my thanks to Ms. Pooja for her companionship and suggestions throughout the course of work.

I like to express my thanks to all the faculties and staffs of the Department of Physics, Bharata Mata College Thrikkakara Kochin Kerala for their support and valuable suggestions that helped me to complete this on time.

I am grateful to my parents, without their love, prayers, sacrifices, and motivation this project would not have been possible. I thank all my friends & others who make the suggestions and feedback towards my project which indeed helped me to complete my project with great success.

Thank you all for your cooperation and kind hearted support.

REFERENCE

1. Biswaranjan Dikshit, Archana Sharma, “Design and Analytical Evaluation of a New Ion Collection Geometry for Improvement in Quantity and Quality of Product During Laser Isotope Separation”, IEEE Transactions on Nuclear Science, VOL. 67, NO.12, pp.2465-2473, December 2020.
2. S. Baruah, B. Jana, A. Majumdar, G.K. Sahu, K.B. Thakur, A.K. Das, “Ion extraction from a flowing plasma using electrostatic field: Simulation and experiment”, Vacuum, VOL 109, pp. 78-81, November 2014.
3. “Beam Technology Development in BARC, Laser& Plasma”, Edited by Martin Mascarenhas, Archana Sharma, pp.154-178,2022.
4. Asawari D. Rath*, A. K. Singh, A. Khattar, A. Wahid, Diptimayee Biswal, A. U. Seema, Ayentika Sen, J. S. B. Singh, S. K. Maurya, J. Thomas, T. Garg, S. Baruah, B. Jana, Dev Ranjan Das, Anupama Prabhala, G. K. Sahu, B. Dikshit, Sanjay Sethi and S. Kundu*, “Laser based Isotope Selective Photoionization for Enrichment of ^{176}Yb, ^{174}Yb and ^{168}Yb”, BARC newsletter, pp.13-17, March-April 2022.
5. Priti Singh, Namita Maiti, “Investigation on Ion extraction processes in M-Type electrode configuration and the influence of top electrode”, Phy. Scr. 99 025609, IOP Publishing, pp.1-11,17 January 2024.
6. C K Birdsall, A B Langdon, “Plasma Physics via Computer Simulation”, IOP Publishing, pp. 3-54, 1991.
7. Asawari D. Rath*, S. Kundu, “Novel Highly Selective Photoionization Scheme for Enrichment of Lu-176”, BARC newsletter, pp.1-5, March-April 2020.
8. Wojciech Konior*, “Particle-in-Cell Electrostatic Numerical Algorithm”, Transactions of the institute of aviation, No. 3(248), pp. 24-38,2017.
9. W. V. Vogel[1]& S. C. van der Marck[2]& M. W. J. Versleijen[1], “Challenges and future options for the production of lutetium-177”, European Journal of Nuclear Medicine and Molecular Imaging, 48:2329–2335, 11 May 2021.
10. M.V. Suryanarayana* & M. Sankari, “Laser isotope separation of 176Luthrough of-the-shelf lasers”,2021.http://www.nature.com/scientificreports.

11. "The Electrostatic Particle in Cell (ES-PIC) Method", pp.1-68, November2010. https://www.particleincell.com/2010/es-pic-method/.
12. Francis F. Chen, "Introduction to Plasma Physics and Controlled Fusion", Third Edition, Spinger International Publishing Switzerland, pp. 1-24, 2016.
13. Paul M. Bellen, "Fundamentals of Plasma Physics", Cambridge University Press, pp.133, 2006.
14. R.J. Goldston, P.H. Rutherford, "Introduction to Plasma Physics", Plasma Physics Laboratory Princeton University, pp. 1-17, 1995
15. Richard Fitzpatrick, "Computational Physics", pp. 265-282.
16. "Lutetium Radiopharmaceuticals in Medicine: A Comprehensive Review". https://openmedscience.com/lutetium-radiopharmaceuticals-in-medicine-a-comprehensive-review/.
17. Dr. Sanjay Kumar. "Leap Frog Method and its Application-I", CC05&09, Patna University.
18. Daniel Martin, "Electrostatic PIC simulation of plasmas in one dimension", pp. 2-10, January 2007.
19. K. K. Mishra *, M. Mascarenhas and Archana Sharma, "Analytical Approach to Understand Laser Isotope Separation Process of Yb-176 for Non-Carrier Added (NCA) Radioisotope Lu-177", BARC newsletter, pp. 21-25, March-April 2022
20. "Lutetium-177 PSMA Therapy". https://www.shebaonline.org/treatment/lutetium-177-psma-therapy/.
21. "What are radioisotopes?"https://www.ansto.gov.au/education/nuclear-facts/what-are-radioisotopes.
22. Ashutosh Dash,Maroor Raghavan Ambikalmajan Pillai, Furn F. Knapp, Jr,"Production of 177Lu for Targeted Radionuclide Therapy: Available Options". https://www.ncbi.nlm.nih.gov/pmc/articles/PMC4463871/.
23. [1]Ewa Ibrahim Inusa, [2]Aliyu Umar Sa'ad, [3]Ayanninuola Olatunji Samuel, [3]Liman Muhammad Sanusi, "Particle-in-cell simulation of electrostatic plasma in one dimension",pp.143-147, 2014.https://www.researchgate.net/publication/318949578_Particle-incellsimulationofelectrostaticplasmainonedimension.
24. M.V. Suryanarayana, "Isotope separation of 176Lu a precursor to 177Lu medical isotope using broadband lasers",2021.
25. https://www.iaea.org/topics/nuclear-science/isotopes/radioisotopes.